Radiation Physics and Chemistry 198 (2022) 110194

Contents lists available at ScienceDirect

Radiation Physics and Chemistry

journal homepage: www.elsevier.com/locate/radphyschem

Thermoluminescence and optically stimulated luminescence of Ba-doped Al_2O_3 produced by a modified sol-gel route

Caline O. Santos [a], Bianca F.S. Santos [a], Yara R.R.S. Rezende [b], Anderson M.B. Silva [a], Linda V.E. Caldas [c], Divanizia N. Souza [a], Ronaldo S. Silva [a], Marcos V.S. Rezende [a,*]

[a] Departamento de Física, Universidade Federal de Sergipe, São Cristóvão, SE, Brazil
[b] Laboratório de Flavor, Universidade Federal de Sergipe, 49100-000, São Cristóvão, SE, Brazil
[c] Instituto de Pesquisas Energéticas e Nucleares/Comissão Nacional de Energia Nuclear, São Paulo, Brazil

ARTICLE INFO

Keywords:
Dosimetry
Thermoluminescence
Optically stimulated luminescence
Aluminum oxide

ABSTRACT

This work features the synthesis and characterization of Al_2O_3 phosphors doped with different concentrations of barium. The samples are produced by a modified sol-gel route, with glucose used as a chelating agent. The luminescent response of the phosphors is also evaluated through their thermoluminescence (TL) and optically stimulated luminescence (OSL). These optical properties are characterized with pellets obtained from the addition of Teflon to the phosphors. Through the TL analysis carried out with a heating rate of 10 °C/s, the samples reveal two intense TL glow peaks with different glow curve shapes when varying the dopant concentration of all the samples. By means of the TL emission curves of the pellets, activation energies associated with the transfer processes of the materials are determined. The phosphors present typical exponential OSL decay curves with a predominance of fast and medium components, indicating that the traps have a high photoionization cross section for blue light-emitting diodes.

1. Introduction

Aluminum oxide (Al_2O_3) is a well-known material that exhibits interesting luminescent properties, such as radioluminescence (Erfurt et al., 2000), thermally stimulated luminescence (TL) (Akselrod et al., 1993) and optically stimulated luminescence (OSL) (Akselrod et al., 1993). Furthermore, Al_2O_3 also has excellent mechanical, electrical, thermal and optical properties and is chemically and thermally stable. Benefitting from these properties and its low effective atomic number that is close to soft tissue, Al_2O_3 has become one of the most used dosimeter materials for individual monitoring (Kato et al., 2018). Recent investigations have shown that dosimetric properties are also observed in Al_2O_3 when it is doped with Cr (Ahmed et al., 2018), Si (Mehta and Sengupta, 1976), Ti (Mehta and Sengupta, 1976), Mg (Osvay and Biró, 1980) and Y (Osvay and Biró, 1980).

Among such dopants, carbon-doped aluminum oxide (Al_2O_3:C) is one of the most well-known and efficient materials for TL and OSL dosimeters and is available as a commercial product (TLD-500) (Yukihara and McKeever, 2008). In Al_2O_3, the C dopant contributes to enhancing the generation of defects, such as F and F^+, which act as emission centers and are responsible for the very high luminescence sensitivity of this material (McKeever et al., 1999). Apart from these investigations, several studies on this material doped with Ba ions have also been reported. It is expected that Ba contributes to the modification of the Al_2O_3 structure in order to increase the number of defects in its structure and to improve its luminescence.

Different routes, such as crystal growth techniques, combustion synthesis (Barros et al., 2008), electrochemical routes (Azevedo et al., 2006), sonochemical preparation (Gedanken et al., 2000), solvent evaporation (Azorín et al., 2002), electrochemical routes (Azevedo et al., 2004) and sol-gel routes, have been used to produce Al_2O_3. Among these routes, sol-gel is a good route due to its simplicity and efficiency. The conventional sol-gel route uses alkoxides for the precursor hydrolyzation and condensation. However, this method has been recently modified by the use of different chelating agents (Andrade et al., 2016; Bezerra et al., 2017; da Costa Cunha et al., 2014; Laokul et al., 2011). The sol-gel route assisted by glucose, for example, has been used in order to produce different inorganic compounds with excellent efficiency in the production of different inorganic compounds (Hora et al., 2016; Liu and Xu, 2011; Carvalho et al., 2019; Silva et al., 2020).

* Corresponding author.
E-mail address: mvsrezende@gmail.com (M.V.S. Rezende).

https://doi.org/10.1016/j.radphyschem.2022.110194
Received 2 September 2020; Received in revised form 23 April 2022; Accepted 26 April 2022
Available online 2 May 2022

The present work focuses on the effects of varying the Ba dopant concentrations on the OSL and TL properties of Al_2O_3:Ba oxides through a systematic investigation designed to meet the requirements of a new alternative route to prepare doped alumina materials for dosimetric applications. The samples are produced by the modified sol-gel route using glucose (Carvalho et al., 2019; Hora et al., 2016). A complete dosimetric characterization is currently under investigation and will be reported in the near future.

2. Materials and methods

Al_2O_3 samples doped with different concentrations of Ba ions (x = 0.01, 0.02, 0.03, 0.04, 0.05, 0.06, 0.07 or 0.08) were prepared by the modified sol-gel route using glucose as a chelating agent. Aluminum nitrate ($Al(NO_3)_3.9H_2O$), barium nitrate ($Ba(NO_3)_3$) and glucose were used as starting materials. Initially, the starting materials, in appropriate amounts, were mixed in distilled water. The excess water of the mixture was evaporated on a hot plate until a gelatinous mixture (xerogel) was formed. The xerogel was then annealed at 1000 °C for 2 h. After this annealing, with the resulting white powder, pellets with a 6 mm diameter, 1 mm thickness and 40 mg mass were produced. In order to improve the physical resistance of the pellets, 50% polytetrafluoroethylene (Teflon) in mass was added to the phosphor and then subjected to a uniaxial pressure of 100 kgf by 10 s.

The phase composition of the prepared samples was analyzed by X-ray diffraction (XRD, Advance 8, Bruker) with Cu radiation of λ = 1.54056 Å operating at 40 kV and 40 mA. The XRD analyses showed that the structure of the produced samples corresponds to ICSD 73725 reference number and that the Ba dopant does not contribute to any phase change of Al_2O_3.

To investigate the optical properties, TL and OSL analyses were performed using a Risø TL/OSL reader (Risø National Laboratory, Denmark) with a Hoya U-340 filter immediately after the irradiations. The samples were irradiated with a $^{90}Sr/^{90}Y$ beta source at a dose rate of 81.6 mGy/s of the Risø TL/OSL reader. TL emission curves were obtained using a heating rate of 10 °C/s to a maximum temperature of 400 °C.

For the OSL measurements, the continuous-wave stimulation of blue light-emitting diodes (LEDs) with a peak emission at 470 nm was employed. The signal was collected over 40 s. All the results in this work represent the average of at least three different measurements with the aim of minimizing the uncertainties and ensure the mean batch response of all dosimeters.

3. Results and discussion

Fig. 1 presents the results from XRD for the pure and Ba-doped Al_2O_3 samples. The diffraction patterns present peaks and relative intensities in agreement with their JCPSD 00-042-1468 reference number. It is noteworthy that the Ba dopant does not contribute to any phase change of Al_2O_3. These results suggest that the use of glucose as a chelating agent results in excellent efficiency for the production of Al_2O_3. Based on the peak width, the crystallite sizes (D) of all the samples were calculated using the Scherrer equation.

Fig. 2 shows the TL glow curves of the Ba-doped samples measured after irradiation with an absorbed dose of 1 Gy. A difference between the glow curve shapes of all the samples can be noted and each shows several TL peaks. Among the samples, the 2 mol.% Ba-doped sample exhibited the highest TL intensity, with each sample exhibiting a different TL intensity. These results suggest that different Ba dopant concentrations generated different additional trap centers. Table 1 shows the TL parameters obtained from employing the general kinetic order fitting described by Chen and Mckeever (1997) and Barrera et al. (2019) to determine the kinetic order (b) and activation energy (E) parameters for the two main peaks of the TL emission curves. The method based on numerical computation used some parameters, such as

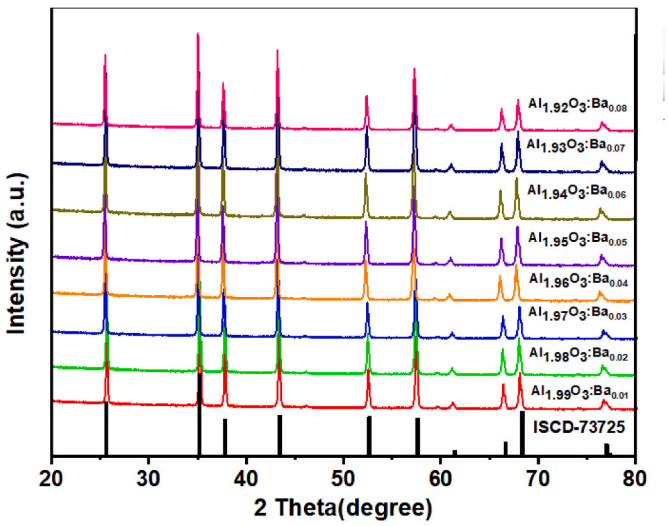

Fig. 1. XRD of Ba-doped Al_2O_3 samples produced by modified sol-gel route.

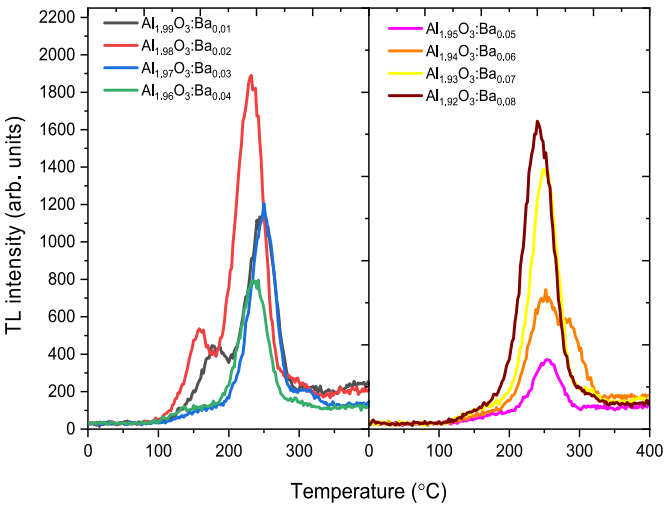

Fig. 2. TL glow curves of Ba-doped Al_2O_3 phosphors irradiated with 1 Gy ($^{90}Sr+^{90}Y$).

the temperature of maximum intensity (T_m) and the maximum intensity of each TL peak (I_m), fixed in the equation by employing OriginLab 8.0 software.

Glow peaks 1 and 2 may be attributed to the $V_{OH}^{-}$and V^{2-} centers, respectively (Kawano et al., 2019). Peak 2 basically agrees well with sol-gel α-Al_2O_3 polycrystalline samples (Ferreira and Santos, 2015). Compared with these reports, our samples showed additional glow peaks. The shift in the glow peak position can be attributed to the difference in the structure caused by the Ba dopant concentration. The Ba dopant substitution in the Al_2O_3 lattice replacing the Al^{3+} ion contributes to the creation of additional defects that induce extra traps. For dosimetric applications, a dosimetric peak should be a single peak at 200–300 °C (McKeever, 2011). Although the thermoluminescent glow curves of the phosphors produced in this work do not present a single peak, the overlapping of the second and third TL peaks results in an emission that can be considered as a main dosimetric peak.

In order to identify the highest TL response to the dose of Al_2O_3 doped with different Ba concentrations, the TL dose response for each concentration was measured as the integrated area under the glow curve (Fig. 3).

Fig. 4 shows the OSL curves with an integration time of 40 s in continuous mode for the samples produced and irradiated with 1 Gy.

Table 1
Maximum glow peak temperature (T_m), maximum intensity (I_m), kinetic order (b) and activation energy (E) of each sample irradiated with 1 Gy ($^{90}Sr+^{90}Y$).

0.01% Ba	Peak 1	Peak 2
T_m (°K)	447.25 ± 2.71	521.37 ± 0.947
I_m (a.u.)	359.17 ± 3.84	1015.41 ± 5.97
Kinetic order (b)	1.01 ± 0.03	1.23 ± 0.10
E (eV)	0.80 ± 0.10	1.01 ± 0.03
0.02% Ba	**Peak 1**	**Peak 2**
T_m (°K)	430.85 ± 0.28	505.09 ± 10.09
I_m (a.u.)	460.39 ± 10.66	1732.47 ± 7.52
Kinetic order (b)	1.36 ± 0.05	1.77 ± 0.09
E (eV)	0.90 ± 0.06	1.36 ± 0.05
0.03% Ba	**Peak 1**	**Peak 2**
T_m (°K)	523.23 ± 0.18	538.75 ± 6.89
I_m (a.u.)	966.02 ± 6.11	196.21 ± 5.44
Kinetic order (b)	1.26 ± 0.03	1.033 ± 0.11
E (eV)	1.62 ± 0.02	0.24 ± 0.01
0.04% Ba	**Peak 1**	**Peak 2**
T_m (°K)	427.34 ± 1.39	509.20 ± 0.030
I_m (a.u.)	93.69 ± 2.53	756.98 ± 10.14
Kinetic order (b)	1.398 ± 0.57	1.683 ± 0.068
E (eV)	0.14 ± 0.065	1.615 ± 0.411
0.05% Ba	**Peak 1**	**Peak 2**
T_m (°K)	445.16 ± 6.14	527.04 ± 0.30
I_m (a.u.)	85.10 ± 2.84	375.49 ± 2 .17
Kinetic order (b)	1.378 ± 0.09	1.4672 ± 0.05
E (eV)	0.146 ± 0.03	1.5640 ± 0.03
0.06% Ba	**Peak 1**	**Peak 2**
T_m (°K)	524.16 ± 0.09	555.02 ± 0.28
I_m (a.u.)	730.87 ± 0.61	591.12 ± 0.16
Kinetic order (b)	1.41 ± 0.55	1.09 ± 0.17
E (eV)	1.29 ± 0.16	0.95 ± 0.19
0.07% Ba	**Peak 1**	**Peak 2**
T_m (°K)	523.9 ± 3.04	579.3 ± 3.69
I_m (a.u.)	1239.63 ± 3.45	153.6 ± 3.65
Kinetic order (b)	1.59 ± 0.09	1.115 ± 0.46
E (eV)	1.51 ± 0.03	0.179 ± 0.01
0.08% Ba	**Peak 1**	**Peak 2**
T_m (°K)	513 ± 0.16	587.5 ± 4.59
I_m (a.u.)	159.2 ± 1.85	186.1 ± 4.18
Kinetic order (b)	1.72 ± 0.06	1.04 ± 0.06
E (eV)	1.42 ± 0.08	0.23 ± 0.09

The results show that the OSL intensity varied considerably from sample to sample, as observed in the TL analyses, and that all the OSL emissions present a typical exponential decay, proving that the traps are emptied during the optical stimulation. Therefore, it may be presumed that the OSL response from these samples is easily stimulated at 470 nm, which indicates that the traps have a high photoionization cross section for blue LEDs. It is noteworthy that these samples present a fast decay rate, which results from the direct recombination between the electrons and holes in the luminescent centers (Silva et al., 2020).

The decay behaviors of the experimental OSL curves can be approximated by three first-order exponential decay functions that were obtained by fitting using the following equation:

$$I_{OSL} = A_1 e^{\frac{-t}{\tau_1}} + A_2 e^{\frac{-t}{\tau_2}} + A_3 e^{\frac{-t}{\tau_3}}$$

where I_{OSL} is the total OSL intensity, A_1, A_2 and A_3 are constant coefficients and τ_1, τ_2 and τ_3 are the decay constants related to the different sets of traps (Valença et al., 2018; Silva et al., 2020). The fitted parameters are listed in Table 2.

The samples present the greatest values for A_1 and A_2, confirming the predominance of OSL decay curves with a fast and a medium component. These OSL emissions, characterized by a fast-initial decay, followed by a slower decay, are evidence of the contribution of trapping centers with different photoionization cross sections (Daniel et al., 2016). The prevalent slow component is minimal, and the greatest fit resulted in $A_3 = 0.29$ and a lifetime of $\tau_3 = 16.7$ s for the OSL response of the analyzed samples.

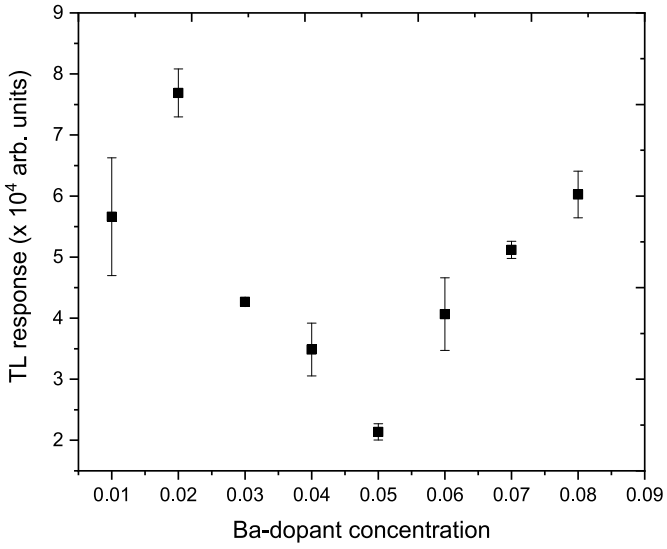

Fig. 3. TL dose response (integrated area) of Al_2O_3 samples doped with different Ba concentrations and irradiated with 1 Gy ($^{90}Sr+^{90}Y$).

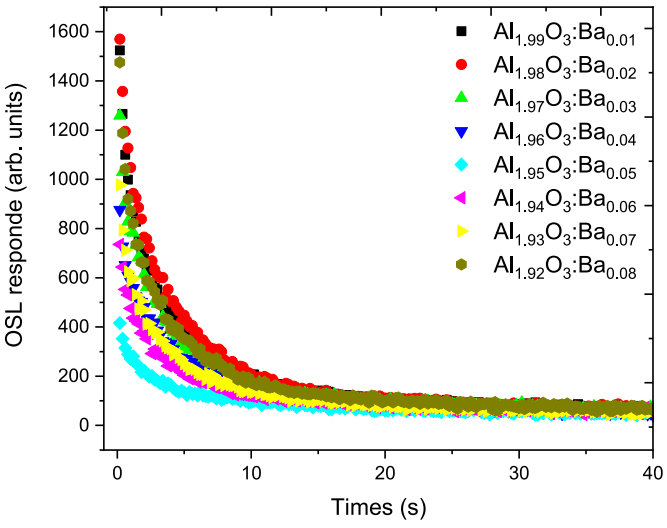

Fig. 4. Typical OSL emission of Ba-doped Al_2O_3 samples irradiated with 1 Gy ($^{90}Sr+^{90}Y$).

The total integrated areas of the OSL curves are shown in Fig. 5. These values are closely related to the TL response. It is possible to note that the OSL response shows the highest intensity for the 0.02% Ba-doped Al_2O_3 and that this result is similar to the one observed for the TL signal.

4. Conclusions

Ba-doped Al_2O_3 samples containing various Ba dopant concentrations were prepared by a modified sol-gel method. The viability of the sol-gel route using glucose as a chelating agent was confirmed. For the eight different samples produced, it was observed that the glow curves consist of peaks with different TL intensities, which are related to the different ratios of Ba as a dopant, which generate additional trapping

Table 2
OSL parameters of the exponential fitted curves of the produced compounds.

Sample	CW-OSL component	Coefficient A_i	Decay constant t_i (s)	Exponential fit
0.01% Ba	Fast	0.54 ± 0.02 (A_1)	0.42 ± 0.02 (t_1)	$R^2 = 0.998$
	Medium	0.55 ± 0.01 (A_2)	3.34 ± 0.14 (t_2)	
	Slow	0.14 ± 0.01 (A_3)	13.61 ± 0.84 (t_3)	
0.02% Ba	Fast	0.43 ± 0.01 (A1)	0.47 ± 0.03 (t_1)	R^2: 0.998
	Medium	0.65 ± 0.01 (A_2)	3.81 ± 0.13 (t_2)	
	Slow	0.09 ± 0.01 (A_3)	16.73 ± 1.44 (t_3)	
0.03% Ba	Fast	0.72 ± 0.08 (A_1)	0.18± 0.02 (t_1)	R^2: 0.997
	Medium	0.67 ± 0.01 (A_2)	3.05 ± 0.09 (t_2)	
	Slow	0.14 ± 0.01 (A_3)	12.89 ± 0.77 (t_3)	
0.04% Ba	Fast	0.66 ± 0.09 (A_1)	0.18 ± 0.02 (t_1)	R^2: 0.997
	Medium	0.66 ± 0.01 (A_2)	3.39 ± 0.10 (t_2)	
	Slow	0.17 ± 0.01 (A_3)	17.38 ± 0.92 (t_3)	
0.05% Ba	Fast	0.55 ± 0.02 (A_1)	0.19 ± 0.06 (t_1)	R^2: 0.989
	Medium	0.57 ± 0.03 (A_2)	2.13 ± 0.17 (t_2)	
	Slow	0.29 ± 0.02 (A_3)	14.59 ± 0.65 (t_3)	
0.06% Ba	Fast	0.46 ± 0.03 (A_1)	0.37 ± 0.05 (t_1)	R^2: 0.994
	Medium	0.62 ± 0.01 (A_2)	3.15 ± 0.16 (t_2)	
	Slow	0.15 ± 0.01 (A_3)	19.22 ± 1.35 (t_3)	
0.07% Ba	Fast	0.60 ± 0.04 (A_1)	0.26 ± 0.02 (t_1)	R^2: 0.996
	Medium	0.59 ± 0.01 (A_2)	2.93 ± 0.12 (t_2)	
	Slow	0.17 ± 0.01 (A_3)	14.39 ± 0.77 (t_3)	
0.08% Ba	Fast	0.62 ± 0.02 (A_1)	0.34 ± 0.02 (t_1)	R^2: 0.997
	Medium	0.57 ± 0.01 (A_2)	3.31 ± 0.12 (t_2)	
	Slow	0.12 ± 0.01 (A_3)	15.30 ± 1.03 (t_3)	

centers. In the case of the OSL response, the phosphors presented a typical exponential decay curve and through the parameters of the exponential fitted curves, the predominance of fast and medium components was confirmed. For the TL glow curves, the phosphors presented OSL emissions with different intensities, which are dependent on the Ba concentrations. These characteristics indicate that these materials present potential use as TL and OSL dosimeters.

CRediT authorship contribution statement

Caline O. Santos: Resources, Formal analysis, Investigation. **Bianca F.S. Santos:** Resources, Formal analysis, Investigation. **Yara R.R.S. Rezende:** Resources, Formal analysis, Investigation. **Anderson M.B. Silva:** Resources, Formal analysis, Investigation. **Linda V.E. Caldas:** Conceptualization, Supervision. **Divanizia N. Souza:** Conceptualization, Methodology, Supervision, Writing – review & editing. **Ronaldo S. Silva:** Conceptualization, Methodology, Supervision. **Marcos V.S. Rezende:** Conceptualization, Methodology, Investigation, Supervision, Writing – review & editing.

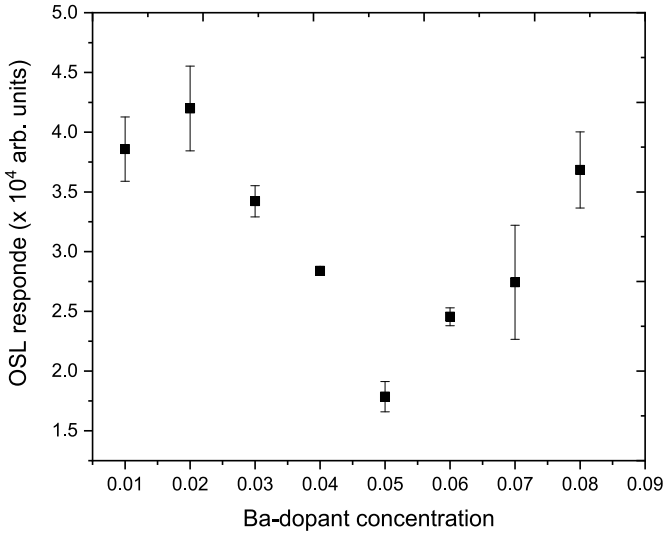

Fig. 5. OSL response (integrated area) of Ba-doped Al_2O_3 samples as a function of dopant sample concentration.

Declaration of competing interest

The authors declare that they have no known competing financial interests or personal relationships that could have appeared to influence the work reported in this paper.

Acknowledgments

The authors are grateful to the Brazilian Funding Agencies: FINEP, CAPES, CNEN and CNPq (407261/2018-4, 308090/2016-0, 308090/2016-0, 427010/2016-0, and 301335/2016-8).

References

Ahmed, M., Salah, A., Ashour, A., Hafez, H., El-Faramawy, N., 2018. Dosimetric properties of Cr doped Al2O3 nanophosphors. J. Lumin. 196, 449–454. https://doi.org/10.1016/j.jlumin.2018.01.001.

Akselrod, M.S., Kortov, V.S., Gorelova, E.A., 1993. Preparation and properties of alpha-Al2O3:C. Radiat. Protect. Dosim. 47, 159–164. https://doi.org/10.1093/oxfordjournals.rpd.a081723.

Andrade, A.B., Ferreira, N.S., Rezende, S., V, M., Hora, D.A., Teixeira, V.C., 2016. Effect of the PVA (polyvinyl alcohol) concentration on the optical properties of Eu-doped YAG phosphors. Opt. Mater. 60, 495–500. https://doi.org/10.1016/j.optmat.2016.09.011.

Azevedo, W., Carvalho, D., Vasconcelos, E., Silva, E., 2004. Photoluminescence characteristics of rare earth-doped nanoporous aluminum oxide. Appl. Surf. Sci. 234, 457–461. https://doi.org/10.1016/j.apsusc.2004.05.147.

Azevedo, W.M., de Oliveira, G.B., Silva, E.F., Khoury, H.J., Oliveira de Jesus, E.F., 2006. Highly sensitive thermoluminescent carbon doped nanoporous aluminium oxide detectors. Radiat. Protect. Dosim. 119, 201–205. https://doi.org/10.1093/rpd/nci684.

Azorín, J., Esparza, A., Falcony, C., Rivera, T., Garcia, M., Martinez, E., 2002. Preparation and thermoluminescence properties of aluminium oxide doped with europium. Radiat. Protect. Dosim. 100, 277–279. https://doi.org/10.1093/oxfordjournals.rpd.a005867.

Barrera, G.R., Souza, L.F., Novais, A.L.F., Caldas, L.V.E., Abreu, C.M., Machado, R., Sussuchi, E.M., Souza, D.N., 2019. Thermoluminescence and optically stimulated luminescence of PbO–H3BO3 and PbO–H3BO3–Al2O3 glasses. Radiat. Phys. Chem. 155, 150–157. https://doi.org/10.1016/j.radphyschem.2018.02.005.

Bezerra, C.S., Andrade, A.B., Montes, P.J.R., Rezende, M.V.S., Valerio, M.E.G., 2017. The effects of cooling rate on the structure and luminescent properties of undoped and doped SrAl2O4 phosphors. Opt. Mater. 72, 71–77. https://doi.org/10.1016/j.jallcom.2015.08.161.

Barros, V.S.M., Azevedo, W.M., Khoury, H.J., Linhares Filho, P., 2008. Combustion synthesis: a suitable method to prepare doped materials for thermoluminescent dosimetry. Radiat. Meas. 43, 345–348. https://doi.org/10.1016/j.radmeas.2007.11.040.

Carvalho, I.S., Silva, A.J.S., Nascimento, P.A.M., Moulton, B.J.A., Rezende, M.V., dos, S., 2019. The effect of different chelating agent on the lattice stabilization, structural and luminescent properties of Gd3Al5O12:Eu3+ phosphors. Opt. Mater. 98, 109449 https://doi.org/10.1016/j.optmat.2019.109449.

Chen, R., Mckeever, S.W.S., 1997. Theory of Thermoluminescence and Related Phenomena. World Scientific, New Jersey.

da Costa Cunha, G., Romão, L.P.C., Macedo, Z.S., 2014. Production of alpha-alumina nanoparticles using aquatic humic substances. Powder Technol. 254, 344–351. https://doi.org/10.1016/j.powtec.2014.01.008.

Daniel, D.J., Raja, A., Madhusoodanan, U., Annalakshmi, O., Ramasamy, P., 2016. OSL studies of alkali fluoroperovskite single crystals for radiation dosimetry. Opt. Mater. 58, 497–503. https://doi.org/10.1016/j.optmat.2016.06.019.

Erfurt, G., Krbetschek, M., Trautmann, T., Stolz, W., 2000. Radioluminescence (RL) behaviour of Al2O3:C-potential for dosimetric applications. Radiat. Meas. 32, 735–739. https://doi.org/10.1016/S1350-4487(00)00052-4.

Ferreira, H.R., Santos, A., 2015. Preparation and characterisation of a sol-gel process -Al2O3 polycrystalline detector. Radiat. Protect. Dosim. 163, 166–172. https://doi.org/10.1093/rpd/ncu143.

Gedanken, A., Reisfeld, R., Sominski, L., Zhong, Z., Koltypin, Y., Panczer, G., Gaft, M., Minti, H., 2000. Time-dependence of luminescence of nanoparticles of Eu[sub 2]O [sub 3] and Tb[sub 2]O[sub 3] deposited on and doped in alumina. Appl. Phys. Lett. 77, 945. https://doi.org/10.1063/1.1289068.

Hora, D.A., Andrade, A.B., Ferreira, N.S., Teixeira, V.C., dos, S., Rezende, M.V., 2016. Effect of the PVA (polyvinyl alcohol) concentration on the optical properties of Eu-doped YAG phosphors. Opt. Mater. 60, 495–500. https://doi.org/10.1016/j.optmat.2016.09.011.

Kato, T., Kawano, N., Okada, G., Kawaguchi, N., Yanagida, T., 2018. Dosimetric properties of Al2O3 transparent ceramics doped with C. Nucl. Instrum. Methods Phys. Res. Sect. B Beam Interact. Mater. Atoms 435, 296–301. https://doi.org/10.1016/j.nimb.2017.12.013.

Kawano, N., Kato, T., Okada, G., Kawaguchi, N., Yanagida, T., 2019. Photoluminescence, scintillation and TSL properties of Eu-doped Al2O3 transparent ceramics synthesized by spark plasma sintering method. Opt. Mater. 88, 67–73. https://doi.org/10.1016/j.optmat.2018.11.002.

Laokul, P., Amornkitbamrung, V., Seraphin, S., Maensiri, S., 2011. Characterization and magnetic properties of nanocrystalline CuFe2O4, NiFe2O4, ZnFe2O 4 powders prepared by the Aloe vera extract solution. Curr. Appl. Phys. 11, 101–108. https://doi.org/10.1016/j.cap.2010.06.027.

Liu, T., Xu, Y., 2011. Synthesis of nanocrystalline LaFeO3 powders via glucose sol-gel route. Mater. Chem. Phys. 129, 1047–1050. https://doi.org/10.1016/j.matchemphys.2011.05.054.

McKeever, S.W.S., 2011. Optically stimulated luminescence: a brief overview. Radiat. Meas. 46, 1336–1341. https://doi.org/10.1016/j.radmeas.2011.02.016.

McKeever, S.W.S., Akselrod, M.S., Colyott, L.E., Agersnap Larsen, N., Polf, J.C., Whitley, V., 1999. Characterisation of Al2O3 for use in thermally and optically stimulated luminescence dosimetry. Radiat. Protect. Dosim. 84, 163–166. https://doi.org/10.1093/oxfordjournals.rpd.a032709.

Mehta, S.K., Sengupta, S., 1976. Gamma dosimetry with Al2O3 thermoluminescent phosphor. Phys. Med. Biol. 21 https://doi.org/10.1088/0031-9155/21/6/006, 006.

Osvay, M., Biró, T., 1980. Aluminium oxide in TL dosimetry. Nucl. Instrum. Methods 175, 60–61. https://doi.org/10.1016/0029-554X(80)90253-0.

Silva, A.M.B., Junot, D.O., Caldas, L.V.E., Souza, D.N., 2020. Structural, optical and dosimetric characterization of CaSO4:Tb, CaSO4:Tb, Ag and CaSO4:Tb,Ag(NP). J. Lumin. 224, 117286 https://doi.org/10.1016/j.jlumin.2020.117286.

Valença, J.V.B., Silva, A.C.A., Dantas, N.O., Caldas, L.V.E., D'Errico, F., Souza, S.O., 2018. Optically stimulated luminescence of the [20% Li2CO3 + x% K2CO3 + (80 - x)% B2O3] glass system. J. Lumin. 200, 248–253. https://doi.org/10.1016/j.jlumin.2018.03.060.

Yukihara, E.G., McKeever, S.W.S., 2008. Optically stimulated luminescence (OSL) dosimetry in medicine. Phys. Med. Biol. 53, R351–R379. https://doi.org/10.1088/0031-9155/53/20/R01.